

UNCLASSIFIED

Defense Technical Information Center  
Compilation Part Notice

ADP011974

TITLE: Adaptive Wavelet Galerkin Methods on Distorted Domains: Setup of the Algebraic System

DISTRIBUTION: Approved for public release, distribution unlimited

This paper is part of the following report:

TITLE: International Conference on Curves and Surfaces [4th], Saint-Malo, France, 1-7 July 1999. Proceedings, Volume 2. Curve and Surface Fitting

To order the complete compilation report, use: ADA399401

The component part is provided here to allow users access to individually authored sections of proceedings, annals, symposia, etc. However, the component should be considered within the context of the overall compilation report and not as a stand-alone technical report.

The following component part numbers comprise the compilation report:

ADP011967 thru ADP012009

UNCLASSIFIED

# Adaptive Wavelet Galerkin Methods on Distorted Domains: Setup of the Algebraic System

Stefano Berrone and Karsten Urban

**Abstract.** We use the algorithm of Bertoluzza, Canuto and Urban [2] for computing integrals of products (of derivatives) of wavelets in order to solve elliptic PDEs on 2D distorted domains. We construct a variant of the original method which turns out to be more efficient. Several numerical results are presented.

## §1. Introduction

Adaptive wavelet Galerkin schemes have quite recently been proven to offer great potential for numerically solving boundary value problems for partial differential equations. On the one hand, strong analytical properties such as convergence and optimal efficiency have been proven for elliptic operators [6,9]. On the other hand, first numerical tests also on non-tensor product domains indicate the applicability of such methods, [1].

However, the major obstacle so far is the efficient computation of the entries of the stiffness matrix and the right-hand side of the corresponding algebraic systems. In fact, it turns out that these entries are more expensive to compute than, e.g., in the case of adaptive Finite Element Methods. In [2], a method to adaptively approximate and compute these entries was introduced and analyzed; numerical results were given for a 1D example. In this paper, we study the application of the algorithm in [2] for 2D ‘distorted’ domains, which are parametric images of the unit square. This allows the study of the influence of ‘realistic’ parametrizations of non-tensor product domains on the assembling of the algebraic system. We incorporate some improvements over the original method in [2] to increase efficiency, and present various numerical results.

## §2. Adaptive Approximation of the Algebraic System

Given a linear boundary value problem in a bounded Lipschitz domain  $\Omega \subset \mathbb{R}^n$  ( $n \geq 1$ ), its numerical approximation by a variational method (Galerkin, Petrov–Galerkin, weighted residuals, ...) requires the computation of integrals of the form

$$\int_{\Omega} b_{\alpha,\beta}(x) D^{\alpha} u(x) D^{\beta} v(x) dx \quad \text{or} \quad \int_{\Omega} f_{\beta}(x) D^{\beta} v(x) dx, \quad (1)$$

where  $\alpha, \beta \in \mathbb{N}^n$  are suitable multi-indices,  $D^{\alpha} = \frac{\partial^{|\alpha|}}{\partial x_1^{\alpha_1} \dots \partial x_n^{\alpha_n}}$  with  $\|\alpha\| := \alpha_1 + \dots + \alpha_n$ ,  $u$  and  $v$  are suitable trial and test functions belonging to  $H^{|\alpha|}(\Omega)$  and  $H^{|\beta|}(\Omega)$  respectively,  $b_{\alpha,\beta} \in L^{\infty}(\Omega)$  and  $f_{\beta} \in L^2(\Omega)$ .

We consider a wavelet Galerkin method with trial and test spaces  $S_{\Lambda} = \text{span } \Psi_{\Lambda}$  generated by adaptively choosing a finite subset  $\Psi_{\Lambda} = \{\psi_{\lambda} : \lambda \in \Lambda\}$  within a wavelet basis  $\Psi = \{\psi_{\lambda} : \lambda \in \mathcal{J}\}$  in  $L^2(\Omega)$ , i.e.,  $\Lambda \subset \mathcal{J}$  (see, e.g., [5,10]). The wavelets are assumed to have the appropriate regularity for the above integrals to be well defined.

The construction of such wavelet bases on fairly general domains  $\Omega$  is not a trivial task. However, quite recently significant progress has been made on this topic, see [3,4,8,12] and also [13] for a somewhat different approach. The main idea behind all the constructions in the first cited papers is domain decomposition and matching. The domain  $\Omega$  is subdivided into  $N$  non-overlapping subdomains  $\Omega_i$ . Each subdomain is mapped to the  $n$ -dimensional reference cube  $\hat{\Omega} := [0, 1]^n$  by means of smooth parametric mappings

$$F_i : \hat{\Omega} \rightarrow \Omega_i, \quad \bar{\Omega}_i = F_i(\hat{\Omega}), \quad G_i := F_i^{-1}. \quad (2)$$

Then, each  $\psi_{\lambda}$ ,  $\lambda \in \mathcal{J}$ , restricted to  $\Omega_i$  is the image through  $F_i$  of a linear combination of tensor product wavelets  $\hat{\psi}_{\hat{\lambda}}$  on  $\hat{\Omega}$ , i.e., if  $\lambda = (j, k)$  ( $j := |\lambda|$  denoting the level and  $k$  the location in space as well as the type of wavelet), then

$$\psi_{\lambda}(x)|_{\Omega_i} = \sum_{\hat{\lambda}' \in S(i,\lambda)} \gamma_{\hat{\lambda}',i} \hat{\psi}_{\hat{\lambda}'}(G_i(x)), \quad x \in \Omega_i,$$

where  $S(i, \lambda)$  is a suitable set of indices of the form  $\hat{\lambda}' = (j, \hat{k}')$  with  $\hat{k}' \in \hat{\Omega}$  and  $\gamma_{\hat{\lambda}',i}$  are suitable coefficients independent of  $j$  (see e.g. [3,4]).

### 2.1. Reduction to univariate integrals

We will only consider the calculation of the integral on the left-hand side of (1) which enters into the stiffness matrix. The entries for the right-hand side are treated analogously, [2]. Hence, replacing  $u$  by  $\psi_{\lambda}$  and  $v$  by  $\psi_{\mu}$  on the left-hand side in (1) for some  $\lambda, \mu \in \Lambda$ , we get

$$\begin{aligned} a_{\lambda,\mu} &:= \int_{\Omega} b_{\alpha,\beta}(x) D^{\alpha} \psi_{\lambda}(x) D^{\beta} \psi_{\mu}(x) dx = \sum_{i=1}^N \sum_{\substack{\alpha' \in T(i,\alpha), \\ \beta' \in T(i,\beta)}} \sum_{\substack{\hat{\lambda}' \in S(i,\lambda), \\ \hat{\mu}' \in S(i,\mu)}} \gamma_{\hat{\lambda}',i} \gamma_{\hat{\mu}',i} \\ &\quad \times \int_{\hat{\Omega}} b_{\alpha,\beta}(F_i(\hat{x})) d_{\alpha'}(\hat{x}) d_{\beta'}(\hat{x}) |JF_i(\hat{x})| \hat{D}^{\alpha'} \hat{\psi}_{\hat{\lambda}'}(\hat{x}) \hat{D}^{\beta'} \hat{\psi}_{\hat{\mu}'}(\hat{x}) d\hat{x}, \quad (3) \end{aligned}$$

where the sets  $T(i, \alpha), T(i, \beta)$  are defined by the chain rule, and  $d_{\alpha'}$  and  $d_{\beta'}$  are smooth functions depending on  $G_i$  and its derivatives. The integrals which appear on the right-hand side of (3) take the form

$$\hat{d}_{\hat{\lambda}, \hat{\mu}} := \int_{\Omega} \hat{c}(x) \hat{D}^{\hat{\alpha}} \hat{\psi}_{\hat{\lambda}}(\hat{x}) \hat{D}^{\hat{\beta}} \hat{\psi}_{\hat{\mu}}(\hat{x}) d\hat{x}, \quad \text{where } \hat{\psi}_{\hat{\lambda}}(\hat{x}) = \prod_{i=1}^n \hat{\theta}_{\hat{\lambda}_i}(\hat{x}_i) \quad (4)$$

and  $\hat{\theta}_{\hat{\lambda}_i}$  are univariate scaling functions or wavelets on  $[0, 1]$ . Now, we use the Two-Scale-Relation for the wavelets to express them in terms of scaling functions on the next higher level, i.e.,

$$\hat{\psi}_{\hat{\lambda}}(\hat{x}) = \sum_{\hat{\Delta} \in \Delta_{\hat{\lambda}}} m_{\hat{\lambda}, \hat{\Delta}} \hat{\varphi}_{\hat{\Delta}}(\hat{x}), \quad (5)$$

where  $m_{\hat{\lambda}, \hat{\Delta}}$  are the refinement coefficients. Here, the index set  $\Delta_{\hat{\lambda}} \subset \mathcal{I}_{|\hat{\lambda}|+1}$  is determined by the Two-Scale-Relation and  $\mathcal{I}_j$  denotes the set of all scaling function indices on a level  $j$ . Hence,  $\hat{d}_{\hat{\lambda}, \hat{\mu}}$  becomes

$$\hat{d}_{\hat{\lambda}, \hat{\mu}} = \sum_{\hat{\Delta} \in \Delta_{\hat{\lambda}}} \sum_{\hat{\underline{\mu}} \in \Delta_{\hat{\mu}}} m_{\hat{\lambda}, \hat{\Delta}} m_{\hat{\underline{\mu}}, \hat{\underline{\mu}}} \int_{\Omega} \hat{c}(x) \hat{D}^{\hat{\alpha}} \hat{\varphi}_{\hat{\Delta}}(\hat{x}) \hat{D}^{\hat{\beta}} \hat{\varphi}_{\hat{\underline{\mu}}}(\hat{x}) d\hat{x}. \quad (6)$$

The computation of each integral on the right-hand side of (6) would be highly efficient if we could reduce it to a product of univariate integrals, but, in general, the function  $\hat{c}$  is *not* a tensor product of univariate functions. However, we can expand it in an appropriate tensor product wavelet basis

$$\hat{\Theta}^* := \left\{ \hat{\theta}_{\hat{\nu}}^* : \hat{\theta}_{\hat{\nu}}^*(\hat{x}) = \prod_{i=1}^n \hat{\theta}_{\hat{\nu}_i}^*(\hat{x}_i), \hat{\nu} \in \hat{\mathcal{J}}^* \right\}, \quad (7)$$

(where  $\hat{\theta}_{\hat{\nu}_i}^*$  are again univariate scaling functions and wavelets on  $[0, 1]$ , respectively, possibly different from  $\hat{\theta}_{\hat{\nu}_i}$ ) as follows

$$\hat{c}(\hat{x}) = \sum_{\hat{\nu} \in \hat{\mathcal{J}}^*} c_{\hat{\nu}} \hat{\theta}_{\hat{\nu}}^*(\hat{x}). \quad (8)$$

Then, we approximate  $\hat{c}$  locally on  $S_{\hat{\lambda}, \hat{\underline{\mu}}} := \text{supp } \hat{\varphi}_{\hat{\lambda}} \cap \text{supp } \hat{\varphi}_{\hat{\underline{\mu}}}$  by a finite sum  $\hat{Q}_{\Lambda} \cdot \hat{c}$ , obtained by restricting the sum in (8) to a finite index set  $\Lambda^* \subset \hat{\mathcal{J}}^*$  (depending on  $\hat{c}$  as well as on  $\hat{\alpha}, \hat{\beta}, \hat{\lambda}, \hat{\underline{\mu}}, \hat{\Delta}$  and  $\hat{\underline{\mu}}$ ), whose precise definition will be given below. Correspondingly,  $\hat{d}_{\hat{\lambda}, \hat{\underline{\mu}}}$  is approximated by

$$\hat{d}_{\hat{\lambda}, \hat{\underline{\mu}}}^* := \sum_{\hat{\Delta} \in \Delta_{\hat{\lambda}}} \sum_{\hat{\underline{\mu}} \in \Delta_{\hat{\underline{\mu}}}} m_{\hat{\lambda}, \hat{\Delta}} m_{\hat{\underline{\mu}}, \hat{\underline{\mu}}} \int_{\Omega} \hat{Q}_{\Lambda} \cdot \hat{c}(\hat{x}) \hat{D}^{\hat{\alpha}} \hat{\varphi}_{\hat{\Delta}}(\hat{x}) \hat{D}^{\hat{\beta}} \hat{\varphi}_{\hat{\underline{\mu}}}(\hat{x}) d\hat{x}, \quad (9)$$

which is a finite linear combination of products of univariate integrals of the following form

$$\int_0^1 \hat{\theta}_{\hat{\nu}_i}^*(\hat{x}_i) \hat{\theta}_{\hat{\lambda}_i}^{(\hat{\alpha}_i)}(\hat{x}_i) \hat{\theta}_{\hat{\mu}_i}^{(\hat{\beta}_i)}(\hat{x}_i) d\hat{x}_i, \quad i = 1, \dots, n. \quad (10)$$

An algorithm for computing such integrals can be found in [2]. However, here we use biorthogonal B-spline wavelets [7,11] as trial and test functions. Due to their explicit representation, efficient direct formulas for the integrals (10) are available and have been used for the subsequent numerical experiments.

Let us mention that the above strategy slightly differs from [2] since here we approximate  $\hat{c}$  locally on  $S_{\hat{\lambda}, \hat{\mu}}$ , whereas in [2] this is done on the somewhat larger domain  $S_{\hat{\lambda}, \hat{\mu}} := \text{supp } \hat{\psi}_{\hat{\lambda}} \cap \text{supp } \hat{\psi}_{\hat{\mu}}$ . This new method ensures automatically that only non-zero integrals are computed, avoiding a wide number of checks, which explains why the present method is more efficient than the original one.

## 2.2. Adaptive approximation of the stiffness matrix

Now, we are going to describe the construction of the index set  $\Lambda^*$  introduced above. To this end, we have to introduce some notation. Let us set

$$\mathcal{I}(\hat{\lambda}, \hat{\mu}) := \{\hat{\nu} \in \hat{\mathcal{J}}^* : |\text{supp } \hat{\theta}_{\hat{\nu}}^* \cap \text{supp } \hat{\varphi}_{\hat{\lambda}} \cap \text{supp } \hat{\varphi}_{\hat{\mu}}| > 0\}, \quad (11)$$

and  $j := \min\{|\hat{\lambda}|, |\hat{\mu}|\}$  as well as  $J := \max\{|\hat{\lambda}|, |\hat{\mu}|\}$ . Let  $R_{\hat{\nu}}$  be the number of zero moments of  $\hat{\theta}_{\hat{\nu}}^*$ , [5,10]. Moreover, let  $T_{\hat{\lambda}}$  and  $T_{\hat{\mu}}$  be the largest integers such that  $\hat{\varphi}_{\hat{\lambda}} \in W^{T_{\hat{\lambda}}, \infty}(\hat{\Omega})$  and  $\hat{\theta}_{\hat{\nu}}^* \in W^{T_{\hat{\nu}}, \infty}(\hat{\Omega})$ , respectively. Then, we set

$$R := \min\{R_{\hat{\nu}}, T_{\hat{\lambda}} - \|\hat{\alpha}\|, T_{\hat{\mu}} - \|\hat{\beta}\|\}.$$

We make the following

**Assumption 1.** *The system  $\hat{\Theta}^*$  defined in (7) allows the characterization of the Besov space  $B_{q,q}^\sigma(\hat{\Omega})$  for indices  $(\sigma, q)$  in a certain range  $\mathcal{S}_{\Theta^*} \subseteq \mathbb{R}^+ \times (0, 1]$ , i.e., the Besov seminorm  $|\cdot|_{B_{q,q}^\sigma(\hat{\Omega})}$  has the representation*

$$|\hat{v}|_{B_{q,q}^\sigma(\hat{\Omega})} \sim \left( \sum_{\hat{\nu} \in \hat{\mathcal{J}}^*} 2^{|\hat{\nu}| \sigma q} 2^{|\hat{\nu}| n(q/2-1)} |\hat{v}_{\hat{\nu}}|^q \right)^{1/q}, \quad \hat{v} \in B_{q,q}^\sigma(\hat{\Omega}). \quad (12)$$

The following notation will be frequently used in the sequel. For  $\ell = 1, \dots, L$ , we consider (possibly different) wavelet bases  ${}_\ell \Psi = \{{}_\ell \psi_{\lambda_\ell} : \lambda_\ell \in {}_\ell \mathcal{J}\}$ . Then, for  $\lambda_\ell \in {}_\ell \mathcal{J}$ ,  $\ell = 1, \dots, L$ , we define

$$i(\lambda_1, \dots, \lambda_L) := \begin{cases} 1, & \text{if } |\bigcap_{\ell=1}^L \text{supp } {}_\ell \psi_{\lambda_\ell}| > 0, \\ 0, & \text{otherwise.} \end{cases}$$

Now, we are in a position to define the set  $\Lambda^*$ . Let us fix, once and for all, independently of  $\hat{\lambda}$  and  $\hat{\mu}$ , a non-increasing  $\ell^1(N_0)$ -sequence  $\delta = (\delta_\ell)_{\ell \in N_0}$  with strictly positive elements, whose  $\ell^1(N_0)$ -norm is close to 1. Let  $\hat{c} \in B_{q,q}^\sigma(\hat{\Omega})$  for some  $(\sigma, q) \in \mathcal{S}_{\Theta^*}$ . For an index  $\hat{\nu} \in \hat{\mathcal{J}}^*$ , we define its relevance for the computation of  $\hat{c}_{\hat{\nu}} \int_{\hat{\Omega}} \hat{\theta}_{\hat{\nu}}(\hat{x}) \hat{D}^{\hat{\alpha}} \hat{\varphi}_{\hat{\lambda}}(\hat{x}) \hat{D}^{\hat{\beta}} \hat{\varphi}_{\hat{\mu}}(\hat{x}) d\hat{x}$  as

$$\begin{aligned} \rho_{\hat{\lambda}, \hat{\mu}}^{(\hat{\alpha}, \hat{\beta})}(\hat{\nu}) := & i(\hat{\lambda}, \hat{\mu}, \hat{\nu}) 2^{-|\hat{\nu}| \sigma q} 2^{-|\hat{\nu}| n(q/2-1)} |\hat{c}_{\hat{\nu}}|^{1-q} \\ & \times 2^{-(R+n/2)(|\hat{\nu}|-J)} 2^{nJ/2} 2^{|\hat{\lambda}|(\|\hat{\alpha}\|-s)} 2^{|\hat{\mu}|(\|\hat{\beta}\|-s)} \delta_{\|\hat{\lambda}\|-\|\hat{\mu}\|}^{-1}. \end{aligned}$$

Finally, for any  $\varepsilon > 0$ , we define

$$\Lambda^* := \{\hat{\nu} \in \mathcal{I}(\hat{\lambda}, \hat{\mu}) : \rho_{\hat{\lambda}, \hat{\mu}}^{(\hat{\alpha}, \hat{\beta})}(\hat{\nu}) \geq \varepsilon / (m_{\hat{\lambda}, \hat{\lambda}} m_{\hat{\mu}, \hat{\mu}} \# \Delta_{\hat{\lambda}} \# \Delta_{\hat{\mu}}) \text{ or } |\hat{\nu}| \leq J\}, \quad (13)$$

which concludes the construction of an adaptive approximation  $\hat{d}_{\lambda, \mu}^*$  of  $\hat{d}_{\lambda, \mu}$ .

**Remark 2.** The construction of  $\Lambda^*$  according to (13) seems to require the explicit knowledge of all the (infinite) coefficients  $\hat{c}_{\hat{\nu}}$  of  $\hat{c}$ . However, one can estimate a priori a level  $J_\varepsilon$  such that  $\rho_{\hat{\lambda}, \hat{\mu}}^{(\hat{\alpha}, \hat{\beta})}(\nu) < \varepsilon / (m_{\hat{\lambda}, \hat{\lambda}} m_{\hat{\mu}, \hat{\mu}} \# \Delta_{\hat{\lambda}} \# \Delta_{\hat{\mu}})$ , if  $|\nu| > J_\varepsilon$ . Following [2] it is easy to show that this is valid for

$$J_\varepsilon := \left\lceil \frac{\varrho_\varepsilon}{R + \sigma + n(1 - \frac{1}{q})} \right\rceil, \quad (14)$$

where we have set

$$\begin{aligned} \varrho_\varepsilon := & |\log_2 \varepsilon / (m_{\hat{\lambda}, \hat{\lambda}} m_{\hat{\mu}, \hat{\mu}} \# \Delta_{\hat{\lambda}} \# \Delta_{\hat{\mu}})| + (R + n)J + |\hat{\lambda}|(|\hat{\alpha}| - s) \\ & + |\hat{\mu}|(|\hat{\beta}| - s) + \log_2(|\hat{c}|_{B_{q,q}^\sigma(\hat{\Omega})}^{1-q} \delta_{\|\hat{\lambda}\|-\|\hat{\mu}\|}^{-1}) + \log_2 \text{Const}. \end{aligned}$$

Replacing  $d_{\lambda, \mu}$  in the computation of  $a_{\lambda, \mu}$  in (3) by  $d_{\lambda, \mu}^*$  results in an adaptive approximation  $a_{\lambda, \mu}^*$  of  $a_{\lambda, \mu}$ . As already mentioned, one can construct an adaptive approximation  $f_\lambda^*$  for the entry of the right-hand side  $f_\lambda := \int_{\Omega} f_\beta(x) D^\beta \psi_\lambda(x) dx$  in the same way.

### 2.3. Error estimates

Let us assume that the boundary value problem we aim at approximating is elliptic of order  $2s$ . Let  $H_b^s(\Omega)$  be the closed subspace of  $H^s(\Omega)$  which accounts for the given boundary conditions. The wavelet basis  $\Psi$  introduced above is assumed to form a Riesz basis of this space. The wavelet Galerkin approximation of our problem is obtained by replacing  $H_b^s(\Omega)$  by  $S_\Lambda := \text{span}\{\psi_\lambda : \lambda \in \Lambda\}$ , where again  $\Lambda$  is an adaptively chosen subset of  $\mathcal{J}$ . The corresponding Galerkin solution will be denoted by  $u_\Lambda := \sum_{\lambda \in \Lambda} u_\lambda \psi_\lambda$ . The vector  $\mathbf{u}_\Lambda := (u_\lambda)_{\lambda \in \Lambda}$  is obtained by solving the linear algebraic system

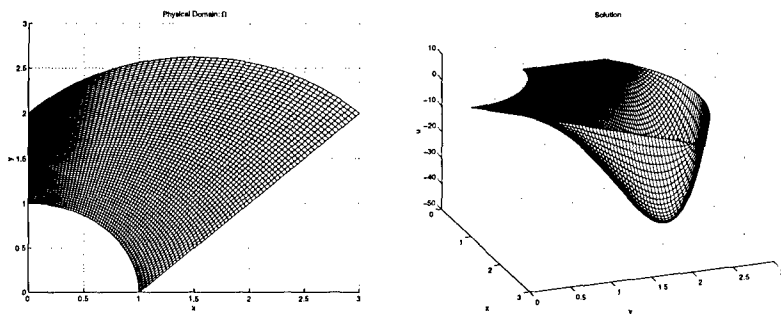


Fig. 1. Physical domain (left) and exact solution (right) for the numerical tests.

$\mathbf{A}_\Lambda \mathbf{u}_\Lambda = \mathbf{f}_\Lambda$ , which is defined in a straightforward manner. Let the integrals which appear in the stiffness matrix as well as the right-hand side be computed in an approximate way, as described above. Denote the resulting matrix by  $\mathbf{A}_\Lambda^*$  and the resulting vector by  $\mathbf{f}_\Lambda^*$ ; let  $\mathbf{u}_\Lambda^*$  be the solution of the modified linear system  $\mathbf{A}_\Lambda^* \mathbf{u}_\Lambda^* = \mathbf{f}_\Lambda^*$  and let  $u_\Lambda^* = \sum_{\lambda \in \Lambda} u_\lambda^* \psi_\lambda$ .

The following estimate on the effect of the described approximation of the stiffness matrix and the right-hand side has been established in [2]. It is readily seen that it also holds for our variant of the original method in [2].

**Theorem 3.** *Under the above and similar assumptions for computing the right-hand side, there exists  $\varepsilon_0 > 0$  such that for all  $0 < \varepsilon \leq \varepsilon_0$ :*

$$\frac{|u_\Lambda - u_\Lambda^*|_{s,\Omega}}{|u_\Lambda|_{s,\Omega}} \lesssim \varepsilon. \quad \square \quad (15)$$

### §3. Numerical Results

In this section, we present our numerical results. We consider the Poisson problem with homogeneous Dirichlet boundary conditions on a domain  $\Omega$  which is the parametric image of  $\hat{\Omega}$  under a suitable transformation. The domain is displayed in Figure 1, left. The boundary of  $\Omega$  consists of two straight lines and two curved parts. We computed the parametrization of the four parts of the boundary and then the parametric mapping  $F : \hat{\Omega} \rightarrow \Omega$  is determined by *transfinite interpolation*, [14].

We constructed a solution  $u$  which satisfies the boundary conditions and which has a strong layer near the upper right corner of the domain. This function is shown on the right in Figure 1. Since we have an explicit formula for  $u$ , we determined the right-hand side  $f$  by using MAPLE V.

The choice of these parameters allows us to test an interesting situation. Indeed, the parametric mapping is obviously far from being a tensor product. Hence, we can study the influence of a ‘realistic’ transformation. Even though this influence was studied in [2] in 1D, we face here a non-tensor product situation for the first time. Moreover, for computing the right-hand side, two

	$ \lambda  =  \mu  = j_0,$			$ \lambda  = j_0,  \mu  = j_0 + 1$			$ \lambda  =  \mu  = j_0 + 1$		
$\varepsilon$	$J_\varepsilon$	$j_{\max}$	#Int	$J_\varepsilon$	$j_{\max}$	#Int	$J_\varepsilon$	$j_{\max}$	#Int
0.5	5	3, 4	16, 80	8	5, 6	108, 1264	6	4, 5	196, 8150
0.25	5	4	18, 138	8	6	142, 1603	7	5	224, 13168
0.125	5	4, 5	26, 196	8	6, 7	184, 2751	7	5, 6	344, 18052
0.0625	7	4, 5	35, 260	10	7	281, 3924	8	6	442, 21924
0.03125	8	5, 6	44, 454	11	7, 8	396, 8048	9	6, 7	556, 36600
0.015625	8	6	61, 656	11	8	716, 12044	10	7	840, 49916
0.0078125	9	6, 7	82, 1318	12	8, 9	1152, 27708	11	7, 8	1172, 100464

**Tab. 1.** Estimated and determined maximum level and number of integrals in  $\Lambda^*$ .

kinds of effects are present, namely the parametric mapping and the layer near the corner. We stress that we do not intend to study any particular choice for the adaptive discretization, i.e., the choice of the set  $\Lambda$ . We are primarily interested in the behaviour of the adaptive approximation  $\hat{Q}_\Lambda \cdot \hat{c}$  in a realistic situation.

As trial and test functions we used the biorthogonal B-spline wavelets on the interval corresponding to the parameters  $d = \tilde{d} = 2$  (i.e., piecewise linear primal functions and dual functions of lowest possible order) from [11] (see also [7] for the original construction on  $\mathbb{R}$ ). For the system  $\hat{\Theta}^*$ , we choose as in [2] piecewise linear interpolatory wavelets. This of course implies that the computation of the corresponding wavelet coefficients  $c_\nu$  can easily be performed. Moreover, since piecewise linear interpolatory wavelets are nothing else than hierarchical B-splines, the integrals in (10) actually only contain scaling functions.

We used the parameters  $\sigma = 2$ ,  $q = 3/4$ ,  $\delta_k := (k+1)^{-2}$  as well as the corresponding parameters  $\tau = 2$ ,  $p = 3/4$  and  $\bar{\delta}_k := k^{-1}$  for the right-hand side, [2].

In the 1D tests in [2], the parameter  $\varepsilon$  was chosen as the error in the  $H^1$ -norm of a corresponding uniform discretization. From a practical point of view, this is of course unrealistic. First of all, the solution is in general not known. Moreover, the ultimate goal of an adaptive scheme is to avoid a (high level) uniform discretization but to use the degrees of freedom in a more economical way. Hence, we performed various tests on the choice of the parameter  $\varepsilon$ .

Our first test concerns  $J_\varepsilon$  in Remark 2 and the number of integrals needed for computing the elements of the stiffness matrix. Our computations are performed in this way: at first, we start from the minimum level ( $j_0 = 3$ ) for the used wavelet basis, where we fix a certain  $\varepsilon$ , then we solve the problem with scaling functions and wavelets. In Table 1 we compare the theoretical estimate  $J_\varepsilon$  on the maximum level in  $\Lambda^*$  with the values that were actually



determined by our indicators in (13). For different portions of the stiffness matrix, we display the predicted  $J_\varepsilon$ , the detected maximum levels by the indicator as well as the minimum and maximum number of integrals needed for computing non zero-entries.

We see that the estimated  $J_\varepsilon$  is always larger than the effectively used maximum level. This is what we expected, but the efficiency of the algorithm may be reduced by an excessive over-estimate of  $J_\varepsilon$ . We also deduce that the efficiency of the method crucially depends on the choice of  $\varepsilon$  since the number of integrals strongly grows for decreasing  $\varepsilon$ . This is surely due to the low order of the interpolatory wavelets used.

Next, we present in Table 2 the average number of integrals computed for the stiffness matrix and the right-hand side for the first two levels with the same  $\varepsilon$  of Table 1. Here  $J_\Lambda := \max\{|\lambda| : \lambda \in \Lambda\}$ .

$\varepsilon$		0.5	0.25	0.125	0.0625	$3.1e-2$	$1.6e-2$	$7.8e-3$
A	$J_\Lambda = 3$	4.04	5.47	8.57	11.05	16.99	24.15	41.62
	$J_\Lambda = 4$	111.55	48.31	234.08	305.98	489.47	738.67	1336.59
f	$J_\Lambda = 3$	9	9	11.49	17.98	31.27	55.69	95.10
	$J_\Lambda = 4$	87.4	87.4	87.94	90.17	137.56	207.72	411.61

Tab. 2. Average number of integrals per entry.

We deduce that the choice of  $\varepsilon$  not only influences the maximal and minimal number of integrals as shown in Table 1. Since the average number of integrals grows when  $\varepsilon$  decreases, the choice of  $\varepsilon$  effects the efficiency of the computation of the *whole* stiffness matrix. Moreover, the presence of the first wavelet level also increases the number of integrals.

Finally, we consider the error in the  $H^1$ -norm and the relative error

$$r_\Lambda^{\text{ex}} := \frac{|u_\Lambda^* - u|_{1,\Omega}}{|u|_{1,\Omega}}$$

for different choices of the parameter  $\varepsilon$ . In Table 3 and Figure 2 ‘rate’ corresponds to the rate of convergence w.r.t. the exact solution in the  $H^1$ -norm for the first two levels in  $\Lambda$ . We see that these quantities do not depend on  $\varepsilon$ . At these levels the relative discretization error still exceeds the relative error (15). This explains why the rate of convergence is basically constant w.r.t. the choices of  $\varepsilon$ .

Hence, the choice of  $\varepsilon$  matters only if this value is at least of the same order than the relative discretization error. We remark that also for increasing  $\varepsilon$  all scaling functions on level  $J$  whose support overlap  $S_{\hat{\Delta}, \hat{\mu}}$  belong to  $\Lambda^*$ . This implies that the error due to the approximation of the entries of the linear system is bounded.

$\varepsilon$	rate	$r_{\Lambda}^{\text{ex}}$
0.5	1.9666	0.1335
0.25	1.9633	0.1337
0.125	1.9538	0.1344
0.0625	1.9658	0.1338
0.03125	1.9563	0.1343
0.015625	1.9591	0.1342
0.0078125	1.9568	0.1343

Tab. 3. Relative error and rate of convergence in dependence of  $\varepsilon$ .

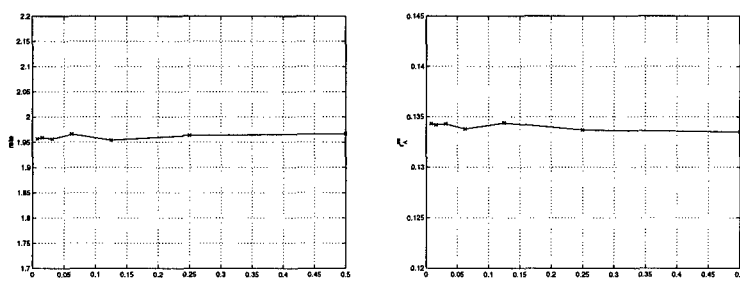


Fig. 2. Rate (left) and  $r_{\Lambda}^{\text{ex}}$  (right) of Table 3.

**Acknowledgments.** We thank Claudio Canuto very much for his helpful advice during the preparation of this paper. The first author is extremely grateful to the Dipartimento di Matematica of the Politecnico di Torino for using its facilities. This work was supported by the *European Commission* within the TMR project (Training and Mobility for Researchers) *Wavelets and Multiscale Methods in Numerical Analysis and Simulation*, No. ERB FMRX CT98 0184. This paper was partly written when the second author was in residence at the Istituto di Analisi Numerica del C.N.R. in Pavia, Italy.

## References

1. Barinka, A., T. Barsch, P. Charton, A. Cohen, S. Dahlke, W. Dahmen, and K. Urban, Adaptive wavelet schemes for elliptic problems — Implementation and numerical experiments, RWTH Aachen, IGPM Preprint 173, 1999.
2. Bertoluzza, S., C. Canuto, and K. Urban, On the adaptive computation of integrals of wavelets, Preprint No. 1129, Istituto di Analisi Numerica del C.N.R. Pavia, 1999. To appear in Appl. Numer. Math.
3. Canuto, C., A. Tabacco, and K. Urban, The wavelet element method, part I: Construction and analysis, Appl. Comp. Harm. Anal. **6** (1999), 1–52.

4. Canuto, C., A. Tabacco, and K. Urban, The wavelet element method, part II: Realization and additional features in 2d and 3d. Preprint 1052, Istituto di Analisi Numerica del C.N.R., Pavia, 1997. To appear in Appl. Comp. Harm. Anal.
5. Cohen, A., Wavelet methods in numerical analysis, in *Handbook of Numerical Analysis*, North Holland, Amsterdam, to appear.
6. Cohen, A., W. Dahmen, and R. DeVore, Adaptive wavelet schemes for elliptic operator equations – Convergence rates, RWTH Aachen, IGPM Preprint 165, 1998.
7. Cohen, A., I. Daubechies, and J.-C. Feauveau, Biorthogonal bases of compactly supported wavelets, *Comm. Pure and Appl. Math.* **45** (1992), 485–560.
8. Cohen, A., and R. Masson, Wavelet adaptive method for second order elliptic problems– boundary conditions and domain decomposition, Preprint, Univ. P. et M. Curie, Paris, 1997, *Numer. Math.*, to appear.
9. Dahlke, S., W. Dahmen, R. Hochmuth, and R. Schneider, Stable multiscale bases and local error estimation for elliptic problems, *Appl. Numer. Math.* **23**, No. 1 (1997), 21–48.
10. Dahmen, W., Wavelet and multiscale methods for operator equations, *Acta Numerica*, **6** (1997), 55–228.
11. Dahmen, W., A. Kunoth, and K. Urban, Biorthogonal spline wavelets on the interval – stability and moment conditions, *Appl. Comp. Harm. Anal.* **6** (1999), 132–196.
12. Dahmen, W., and R. Schneider, Composite wavelet bases for operator equations, *Math. Comput.* **68** (1999), 1533–1567.
13. Dahmen, W., and R. Schneider, Wavelets on manifolds I: Construction and domain decomposition, RWTH Aachen, IGPM Preprint 149, 1998. To appear in *SIAM J. Math. Anal.*
14. Gordon, W., and C. Hall, Transfinite element methods: blending-function interpolation over arbitrary curved element domains, *Numer. Math.* **21** (1973), 109–129.

Stefano Berrone

Dipartimento di Ingegneria Aeronautica e Spaziale

Politecnico di Torino

Corso Duca degli Abruzzi, 24

10129 Torino, Italy

[sberrone@calvino.polito.it](mailto:sberrone@calvino.polito.it)

Karsten Urban

Institut für Geometrie und Praktische Mathematik

RWTH Aachen

Templergraben 55

52056 Aachen, Germany

[urban@igpm.rwth-aachen.de](mailto:urban@igpm.rwth-aachen.de)